Fire-generated smoke rollback through crosscut from return to intake – experimental and CFD study

G.F. Friel, L. Yuan, J.C. Edwards, & R.A. Franks

National Institute for Occupational Safety and Health, Pittsburgh Research Laboratory, Pittsburgh, PA, USA

ABSTRACT: Two mine-fire experiments were conducted in the National Institute for Occupational Safety and Health's (NIOSH) Safety Research Coal Mine (SRCM) at the Pittsburgh Research Laboratory (PRL) which demonstrated that smoke from diesel-fuel fires of 500 kW and 660 kW heat-release rates in a return airway can develop, without causing a complete air flow reversal, into a roof layer that can migrate upwind forming a counter flow to the primary airflow in a crosscut. Subsequently, smoke can penetrate into an intake airway and create a hazardous atmosphere in the intake airway upwind from the fire. Visibility conditions less than 13 m were created by the smoke in the intake airway downwind from the crosscut. Modeling of the event with a three-dimensional, time-dependent, computational fluid dynamics (CFD) program correctly represented the smoke movement.

1 INTRODUCTION

Smoke rollback in a mine entry from a fire can pose hazardous consequences for mine evacuation, miner rescue, or firefighting. Inhalation of fire-generated and toxic products-of-combustion (POC) can be injurious or fatal to miners. The low visibility associated with smoke impedes safe miner escape and rescue. The greatest hazard of smoke rollback is in fighting fires. Smoke rollback can occur directly upwind in the entry with the fire, or if it penetrates a crosscut, it can be transported downwind in the adjoining airway. If a mine rescue team or firefighting brigade should approach a fire in the fresh air of an intake airway before the fire intensity becomes sufficient to push smoke through a breached crosscut into the intake entry upwind of the mine rescue team or firefighting brigade, these miners could then become enshrouded in low visibility and toxic POC.

Initially the thermal buoyancy forces generated by a fire in a mine entry will produce an ascending plume of fire smoke. In the absence of ventilation, the hot smoke will impinge upon the roof and migrate radially outward. Any entry ventilation will bend the ascending smoke plume. Initially, the dominant transport of the smoke at the roof will be in the direction of the ventilation. The smoke will be transported downwind from the fire along the roof until the smoke is cool and is mixed over the entry cross-section. However,

once the fire has evolved to sufficient intensity, the buoyancy forces associated with the temperature of the smoke plume will overcome the inertial forces of the ventilation, and some of the smoke will migrate upwind along the roof counter to the existing ventilation direction. Another hazard of smoke rollback, noted by Mitchell (1996), is that the smoke can contain combustible gases in a low-oxygen mixture which are subject to ignition by the mine fire when diluted with fresh air.

Previous research (Edwards et al. 2005, Hwang & Edwards 2005) has focused upon smoke rollback in a single entry and the air velocity required to prevent the smoke rollback. For a sufficiently intense fire relative to the airflow, it is possible to develop complete airflow reversal in an airway that can be modeled accurately by a network mine-fire simulator such as MFIRE (Chang et al. 1990).

Smoke rollback in a mine entry can be complicated by the connectivity of the entry to other mine entries by open crosscuts and leakage paths. The smoke layer which accumulates near the roof can migrate into parallel airways depending upon the air velocity and the amount of leakage between the airways. Permanent stoppings are used to separate intake and return airways in a coal mine except for the first two connecting crosscuts outby the working face. A check curtain may be used at the second crosscut outby the working face to provide for vehicular traffic movement. Any breach

of the stoppings due to an open man door or stopping destruction by a fire or explosion, or significant leakage around a stopping or check curtain, creates the potential for smoke flow from a fire in a return airway into an intake airway.

The objective of this work was to demonstrate with in-mine fire experiments the potential for smoke roll-back from a fire in a return airway into an intake airway and to model this experimental work with CFD simulation. CFD provides the opportunity to expand the range of prediction of smoke spread for a wide spectrum of airflows, fire intensities, and mine-section inclinations and layouts.

Figure 1. View of the mine section in the NIOSH SRCM (Not drawn to scale).

2 EXPERIMENTAL CONFIGURATION

Experiments were conducted in parallel entries in the SRCM shown in Figure 1.

The average entry height and width at the location of the fire in B-Butt were 1.81 and 2.79 m, respectively. Diesel fuel was selected as the combustible material for the fires because of its relatively uniform burning rate from containers. The three containers that were used were horizontally square steel pans with sides of 46 cm, 61 cm, and 76 cm long. The heights of the pan sides were about 13 cm. The fire zone was protected from thermal radiation by lining the roof and ribs with a ceramic fiber insulation. The smoke concentration in B-Butt upwind of the fire was measured by an ionization detector at sensor station, S1, near the middle of B-Butt with its inlet about 20 cm from the roof and its position at 15.5 m from the upwind edge of the fire zone and 4.2 m from the upwind edge of Room 11 (See Figure 1). A thermocouple was also placed near the ionization detector and about 8 cm from the roof. A one-meter-long, laser, smoke-obscuration meter (laser-light meter) was also positioned near the ionization detector and 30 cm from the roof. Along the rib of B-Butt at S2 and 12.5 m upwind from the ionization detector was the first of two steel mine posts which supported a pair of path-averaging sensors. The second post was 21.8 m from the ionization detector on the opposite rib of B-Butt. An infrared smoke sensor, composed of a transmitter and a receiver, was attached to the posts about 60 cm from the roof with the infrared beam directed horizontally and diagonally 10.2 m across B-Butt. Two units of a gas-velocity sonic sensor also were attached to these two posts. One unit was attached 20 cm from the roof on the first post and the other unit was attached 30 cm from the floor on the second post. The length of the path between these units was 9.7 m. The gas-velocity sensor units were attached on the sides of the posts closest to each other while the smoke sensor units were attached on the sides farthest from each other.
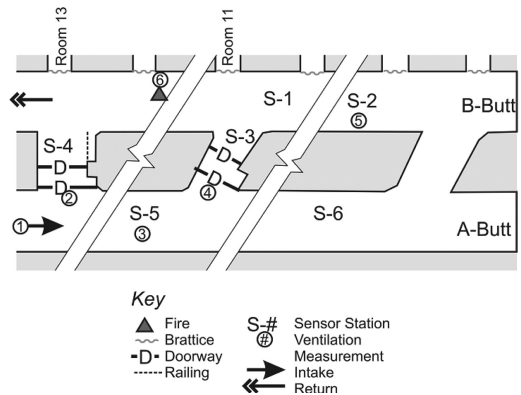
In the crosscut upwind of the fire, Room 11, and 4.8 m from B-Butt, a one-meter-long, optical, smoke-obscuration meter (light meter) was suspended horizontally 30 cm from the roof at S3. A thermocouple was attached 10 cm from the roof above this light meter. The upwind edge of the crosscut downwind from the fire zone, Room 13, was 25 m from the fire zone. Within Room 13, 5.2 m from B-Butt, and at S4 was another light meter 30 cm from the roof. A thermocouple was also placed 10 cm from the roof above this light meter.

In A-Butt, 2 m downwind from Room 13, and at S5 was placed the first of two posts to hold gas-velocity sensor units and optical, smoke sensor units similar to the configuration in B-Butt. The spacing between the gas-velocity units was 8.9 m and the spacing between the smoke sensor units was 9.4 m.

In A-Butt, at 25 m from the downwind edge of Room 11, and at S6 were placed an ionization smoke sensor and a laser-light meter near the middle of A-Butt to detect smoke emanating from either or both of Rooms 11 and 13. The laser-light meter was 30 cm from the roof and the inlet to the ionization smoke sensor was about 20 cm from the roof.

3 EXPERIMENTAL PROCEDURE

The air velocities at the six positions on Figure 1 were measured using a vane anemometer. At positions 1, 3, 5, and 6 the average velocity was measured at each of five points in the cross section of the airway. At positions 2 and 4 the average velocity was measured at each of 3 points in the cross section of the doorways next to A-Butt. These velocity averages were determined by measuring the velocity over at least one cycle length of atmospheric changes to mine

air velocities which usually lasted about 30 s. Cross-sectional areas were calculated from measurements of height and width using an electronic, ultrasonic distance-measuring tool.

The fire pans were placed level, next to each other, and on the floor near the middle of B-Butt in the fire zone. Attached to a laboratory stand next to the pans was a thermocouple positioned horizontally and about 10 cm above the middle of the downwind pan to indicate the end of combustion. The diesel fuel was poured into a measuring container before being poured into each pan. Before ignition of the diesel fuel using a propane torch, about 250 mL of denatured, 95% ethanol was poured into each pan. The cold diesel fuel was difficult to ignite without the ethanol. After ignition, exiting of personnel from B-Butt was through Room 11 into A-Butt and then along A-Butt to a point upwind of Room 13. A digital camcorder was attached to a tripod about 1.5 m from the floor of A-Butt and opposite Room 13 to record the smoke emanating from Room 13 and also Room 11 by pivoting the camcorder 90°.

4 MEASUREMENT OF ROOM RESISTANCES

The static pressure drops between A-Butt and B-Butt through Room 11 and Room 13 were measured using a manometer placed level on a pedestal within the rooms with tubes extended into A and B-Butts. The airflow rates through the rooms were calculated from the average of three velocity measurements at different heights within doorways in each room using the vane anemometer and the dimensions of the doorways. The static pressures were measured using an altimeter. The temperatures and relative humidities were measured using a digital psychrometer. The resistances were calculated by dividing the air static pressure drop by the square of the volumetric airflow rate. The results of those measurements at mine static air pressures and temperatures are listed below in Table 1. The resistances can be converted to a standard set of conditions for use in simulators such as MFIRE.

5 EXPERIMENTAL RESULTS

Table 2 shows the volumetric airflow rates in the mine network prior to each experiment. Also shown are the air velocity measurements at position 1 that were repeated after each experiment because of changes to the airflow rate into A-Butt during each experiment. These velocity changes were made after a semi-equilibrium position of smoke had occurred in Room 13 and to facilitate penetration of smoke into A-Butt before the diesel fuel was all consumed. These ventilation decreases were accomplished by opening a

Table 1. Measured resistances through crosscuts.

Room Number	Resistance, Ns^2/m^8	Static Pressure, cm Hg	Temperature, °C	Relative Humidity, %
11	0.1709	73.56	2.39	89.8
13	0.1407	73.53	1.78	92.6

Table 2. Airflow rates at locations in Figure 1.

Location on Figure 1	Experiment 1 (500 kW Fire) Airflow Rate, m^3/s	Experiment 2 (660 kW Fire) Airflow Rate, m^3/s
1	4.2	4.5
2	1.8	1.6
3	3.2	3.5
4	1.7	1.6
5	2.2	2.4
6	1.7	1.8
1, During Experiments	3.5	3.7

door in a crosscut from A-Butt to the return and upwind of the entrance to Room 13. The airflow rates for the two experiments were similar, although the inaccuracies in the volumetric balances could have been caused by the vortices produced by the edges of nearby rooms and leakage around temporary brattices.

In the first experiment, 23.7 L of diesel fuel was burned in the 46 cm and 61 cm square pans. Based upon the fire duration and the heat of combustion for diesel fuel, the fire intensity was estimated to be 500 kW. A large quantity of smoke passed through Room 11 upwind of the fire and from there downwind through A-Butt and back through B-Butt and the fire zone. This fire yielded no penetration of smoke from B-Butt through Room 13 into A-Butt until a reduction in airflow rate through A-Butt was made. Figure 2 shows the light meter response in millivolts (mV), which decreased with an increase in the concentration of smoke at the light meter, and the temperature at the thermocouple within Room 13 during the first experiment. The POC's penetrated to the doorway next to A-Butt. All sensors were sampled every two seconds. Figure 3 shows the light meter and thermocouple response within Room 11 during the first experiment.

Figure 4 shows the temperature and indicates smoke intensity at the point ionization smoke sensor in B-Butt (S1), and indicates the smoke intensity at the point ionization smoke sensor in A-Butt (S6) located 25 m downwind from Room 11 during the first experiment. About a minute was required for the smoke to backup 12 m.
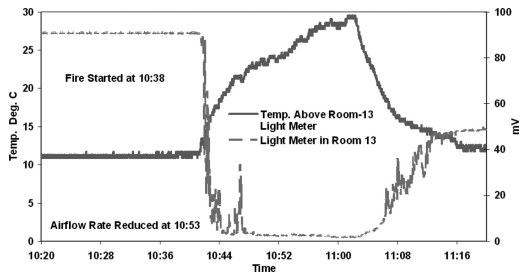
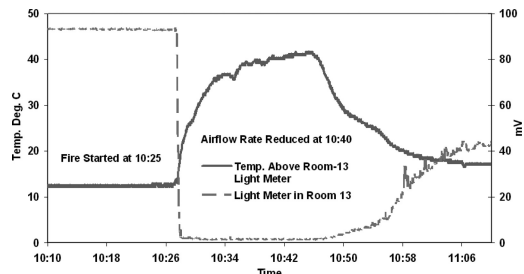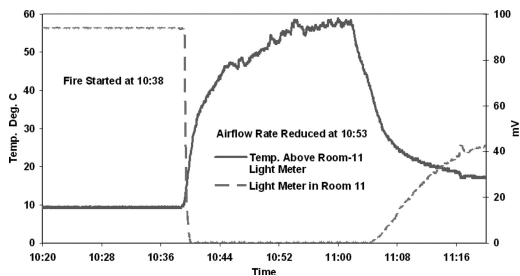Figure 2. Temperature and light meter response in Room 13 for experiment no. 1.

Figure 3. Shows the light meter and thermocouple response within Room 11 during the first experiment.
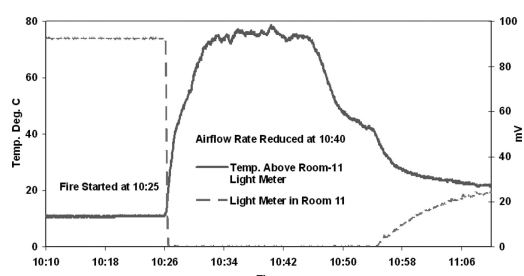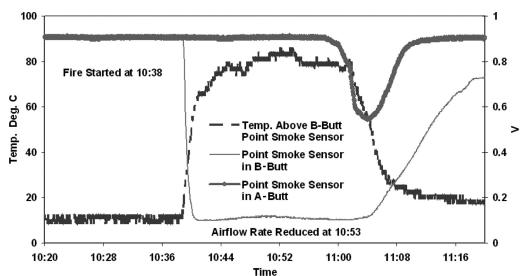

Figure 4. Sensor responses in A-Butt and B-Butt for experiment no. 1.

In the second experiment, 33.1 L of diesel fuel were burned in the 46 cm and 76 cm square pans. The estimated fire intensity was 660 kW. This fire yielded a brief penetration of smoke from B-Butt through Room 13 into A-Butt. A large quantity of smoke also passed through Room 11 upwind of the fire and from there downwind through A-Butt. The quantity of smoke from Room 13 was much less than the quantity of smoke emanating from Room 11 into A-Butt. Figure 5 shows the light-meter response to the smoke and the temperature of the smoke at the thermocouple within Room 13 during the second experiment. These POC's penetrated from Room 13 into A-Butt continuously during the fire after the flow rate through A-Butt was reduced. The greater smoke rollback into Room 11

Figure 5. Temperature and light meter response in Room 13 for experiment no. 2.

Figure 6. Temperature and light meter response in Room 11 for experiment no. 2.

was associated with the maximum roof temperature of 78°C in Room 11 compared with the maximum roof layer temperature of 42°C in Room 13. For the first experiment, the maximum roof-layer temperatures in Rooms 11 and 13 were 59°C and 29°C, respectively.

Figure 6 shows the light-meter response to the smoke and thermocouple measurement of the smoke temperature within Room 11 during the second experiment.

Figure 7 shows the temperature and indicates smoke intensity at the point, ionization smoke sensor in B-Butt and indicates the smoke intensity at the point, ionization smoke sensor in A-Butt located 25 m downwind from Room 11 during the second experiment. The gas temperature may have caused the temporary failure of the thermocouple's electronic interface which also was supported near the roof.

6   VISIBILITY

As the light-meter responses in Figures 2, 3, 5, and 6 show, smoke obscuration is total near the roof within the crosscuts. Smoke movement through Room 11 from the return, B-Butt, into the intake, A-Butt, created a reduced visibility downwind from Room 11 in A-Butt. The visibility was determined from Jin's relationship (Jin 1977), which, in turn, was based upon
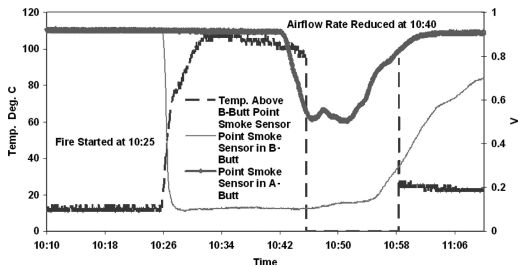
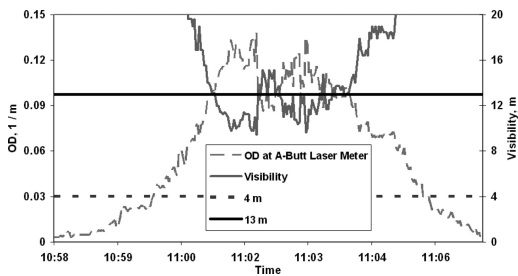Figure 7. Sensor response in A-Butt and B-Butt for experiment no. 2.

Figure 8. Smoke optical density and visibility in A-Butt 25 m downwind from Room 11 during experiment no. 1.

the smoke optical density determined from the reflection of light from a reflecting sign – as might occur when a miner's cap lamp is focused upon a reflecting mine-escape marker. Figure 8 shows the optical density (OD) at the laser light monitor located 25 m downwind from Room 11 and the associated visibility for the 500 kW fire of the first experiment. The optical density is defined from the light transmission at the laser light monitor by equation 1:

$$OD = -1/d \, Log_{10} \, (\, T \, / \, T_0 \,).\qquad(1)$$

T is the light transmission between the transmitter and the receiver in smoke-laden air, T_0 is the light transmission in clear air, and d is the distance between the transmitter and the receiver.

The minimum visibility was 9.4 m. Also shown are the 4 m and 13 m visibility requirements reported by Jin (1981) for minimum visibility of someone familiar and not familiar with the surroundings, respectively. For the 660 kW fire of the second experiment, the minimum visibility was 5.5 m. Someone unfamiliar with the SRCM would not have the minimum visibility for escape from the fire zone through B and A-Butts. A scenario could exist of a firefighting brigade entering B-Butt through A-Butt upwind of the fire zone to extinguish the fire. Initially the fire intensity might not be adequate to force smoke rollback through Room 11 into A-Butt. As the fire intensity increases, the smoke
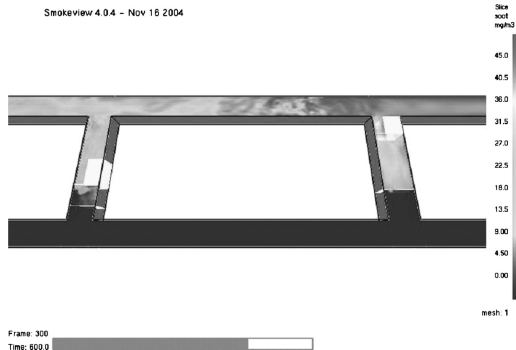

Figure 9. Smoke density distribution near the roof at 600 s for the 500 kW fire.

rollback could not be confined to B-Butt but would penetrate through Room 11 and soon be upwind of the firefighting brigade.

7 COMPUTATIONAL STUDY

Smoke reversal through crosscuts from a return airway into an intake airway was simulated using the Fire Dynamics Simulator (FDS), a CFD program developed by NIST (McGrattan et al. 2002). FDS is a three-dimensional, large-eddy simulation model developed for studying the transport of smoke and hot gases during a fire in an enclosure. It is a widely used large-eddy simulation model in the field of fire science and has demonstrated good agreement with experimental data in numerous validation studies. The model uses finite difference techniques to estimate solutions of the Navier-Stokes equations for fluid flow with a mixture-fraction combustion model.

The physical model for the numerical simulation consists of the intake airway, the return airway, two crosscuts, and an airway connecting the intake and the return airways – as shown in Figure 1. In Figure 9 below the connecting airway was not drawn.

Because of the memory limitations and speed of the computer running FDS, Room 11 was made perpendicular to both intake and return airways to increase the mesh size of the simulation. The two crosscuts each have two doors and a plenum between the doors. All dimensions for the airways and crosscuts were entered from a mine-section survey. Each diesel fire was modeled using its average heat-release rate estimated in the experiment. The airflow velocity measured upwind of Room 13 in A-Butt was entered as the initial flow condition. In both experiments, the airflow velocity was reduced after about 15 minutes from the ignition of the diesel fuel. In the simulation, the smoke movement became quite stable after 10 minutes, so the airflow
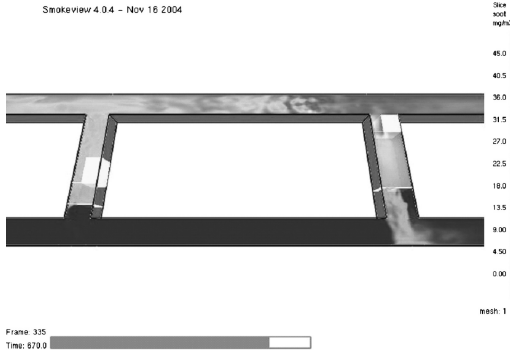
Figure 10. Smoke density distribution near the roof at 670 s for the 500 kW fire.
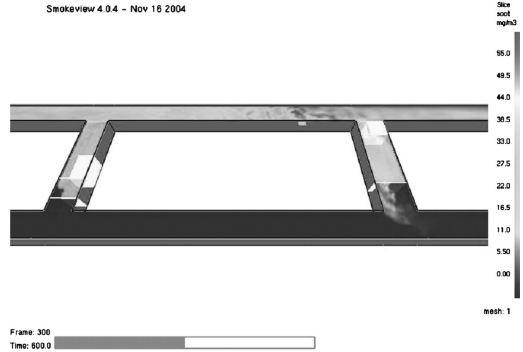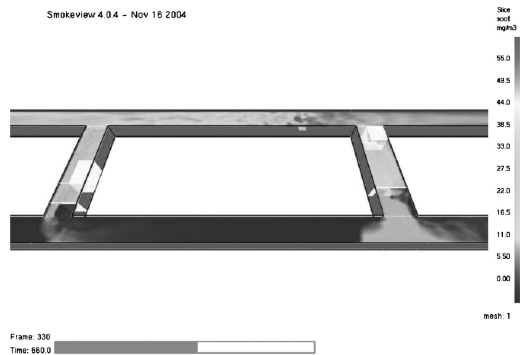

Figure 11. Smoke density distribution near the roof at 600 s for the 660 kW fire.

Figure 12. Smoke density distribution near the roof at 660 s for the 660 kW fire.

velocity change was made after 10 minutes. For the 500 kW fire, the airflow velocity was 0.96 m/s at the beginning and was changed to 0.79 m/s after 10 minutes. For the 660 kW fire, the airflow velocity was 0.99 m/s at the beginning and was changed to 0.80 m/s after 10 minutes.

A cold airflow simulation was conducted prior to the fuel ignition. The airflow rates in A-Butt and the two crosscuts obtained from the simulation agreed well with the rates calculated from the pre-experiment ventilation survey. However, the measured airflow rate in B-Butt was smaller than the simulated rate because of leakage around brattices along one of the ribs in B-Butt into other crosscuts and the rest of the SRCM. Simulations were then conducted for the experimental fires. Figure 9 shows the smoke (soot) density distribution near the roof at 600 s for the 500 kW fire, immediately before the change of the intake air velocity. Smoke passed through the open door of Room 11 adjacent to B-Butt and filled the Room-11 plenum, but could not pass through the open door adjacent to A-Butt. Smoke also passed through the open door of Room 13 adjacent to B-Butt and only partially filled the Room-13 plenum. The smoke inside Room 13 was also less dense than the smoke in Room 11.

Figure 10 shows the smoke density distribution near the roof at 670 s for the 500 kW fire 70 s after the reduction of intake air velocity.

Smoke passed through the open door of Room 11 adjacent to A-Butt and leaked into A-Butt but could not roll upwind in A-Butt. Smoke filled the entire plenum in Room 13 but could not pass through the open door adjacent to A-Butt. As time increased, more smoke leaked into A-Butt from Room 11 and slightly rolled upwind next to the rib closest to Room 11. A small quantity of smoke passed into A-Butt through the open door of Room 13 adjacent to A-Butt. These results are consistent with the observations in the first experiment.

Figure 11 shows the smoke density distribution near the roof at 600 s for the 660 kW fire and immediately before the change of the inlet velocity.

Some smoke already passed into A-Butt from Room 11 through the open door adjacent to A-Butt but was quickly diluted and could not roll upwind in A-Butt. Smoke passed through the open door of Room 13 adjacent to B-Butt and filled most of the plenum.

Figure 12 shows the smoke density distribution near the roof at 660 s for the 660 kW fire 60 s after the ventilation reduction.

Dense smoke leaked into A-Butt from Room 11 and rolled upwind in A-Butt. Smoke filled the entire plenum of Room 13 and less dense smoke leaked into A-Butt. As time increased, more smoke leaked into A-Butt from Room 11 and rolled upwind against the intake airflow, while no more smoke leaked into A-Butt from Room 13. These results also are qualitatively consistent with the observations in the second experiment.

It can be seen from the FDS simulation that the smoke leakage from Room 11 into the A-Butt only occurred near the roof. Close to the floor in Room

11 the ambient air still moved in against the smoke leakage. This is one advantage of the FDS's three-dimensional simulation. In one-dimensional modeling, one airway is either occupied by clear air or an air-smoke mixture but cannot be both. In a real situation partial smoke leakage into an airway could occur and poses a threat to the safety of underground miners and mine rescue personnel.

8 CONCLUSIONS

The following conclusions were determined from the experimental results and the CFD simulations.

- The experimental mine fires in a return airway produced sufficient buoyancy to establish a smoke-laden roof layer that flowed through connecting crosscuts counter to the direction of fresh air from the intake entry.
- The density of the smoke that leaked into the intake was shown to yield insufficient visibility downwind from the last connecting crosscut in the intake entry for someone unfamiliar with the mine to find their way out easily.
- The CFD simulations showed good agreement with the experimental observations of smoke movement.

Smoke rollback along the roof from a fire countercurrent to the cooler airflow near the floor can be a mechanism for smoke to move from a mine return into a mine intake in low airflow sections. This movement of smoke can impede firefighting efforts. The realization of this possibility would not be predicted from a mine-network ventilation program which is based only upon unidirectional flow. CFD modeling is a viable method for analyzing potential visibility hazards associated with smoke from an in-mine fire.

REFERENCES

Chang, X., Laage, L.W. & Greuer, R.E. 1990. A user's manual for MFIRE: a computer simulation program for mine ventilation and fire modeling. *U.S. Bureau of Mines IC 9245*, 171 pp.

Edwards, J.C., Franks, R.A., Friel, G.F. & Yuan, L.L. 2005. Experimental and modeling investigation of the effect of ventilation on smoke rollback in a mine entry. *SME Annual Meeting, Feb 28–Mar 2, 2005, Salt Lake City, UT*, paper 05-14, 6 pp.

Hwang, C.C. & Edwards, J.C. 2005. The critical ventilation in tunnel fires – a computer simulation. *Fire Safety Journal* 40: 213–240.

Jin, T. 1977. Visibility through fire smoke. *Journal of Fire and Flammability* 9: 135–155.

Jin, T. 1981. Studies of emotional instability in smoke from fires. *Journal of Fire and Flammability* 12: 131–142.

McGrattan, K.B., Forney, G.P., Prasad, K., Floyd, J.E. & Hostikka, S. 2002. Fire Dynamics Simulator (Version 3) – User's Guide. U.S. Department of Commerce, National Institute of Standards and Technology.

Mitchell, D.W. 1996. *Mine fires prevention, detection, fighting*: 19-202. Chicago, IL: Intertec Publishing Inc.